AFDM–FMCW Waveform for Low-Complexity Integrated Sensing and Communication via DAFT-Kernel Chirp Embedding

Salman Ahmad, Soo Young Shin

salman@kumoh.ac.kr, wdragon@kumoh.ac.kr

Department of IT Convergence Engineering, Kumoh National Institute of Technology, Gumi, South Korea

Abstract

Integrated sensing and communication (ISAC) must balance sensing accuracy, communication reliability, and receiver complexity. Frequency-modulated continuous-wave (FMCW) radar enables low-complexity analog de-chirping and accurate range–Doppler sensing, while multicarrier waveforms primarily target high-rate links. This paper proposes an affine frequency division multiplexing (AFDM)–FMCW waveform that generates an FMCW-like chirp from selected entries of the inverse discrete affine Fourier transform (DAFT) kernel and preserves chirp continuity under cyclic prefix (CP) insertion. The resulting signal maintains an AFDM communication structure while providing a continuous chirp for analog mixing at the sensing receiver. A unified transmitter/receiver model is presented, supporting DAFT-based demodulation for communications and 2-D FFT range–Doppler processing for sensing. The sensing–communication trade-off is controlled by the chirp-to-data power ratio.

1. Introduction

Future 6G networks increasingly target dual-functional base stations that deliver data while simultaneously sensing the environment, improving spectrum utilization and reducing duplicated hardware. A persistent challenge is that high-rate communication waveforms and radar-friendly waveforms often pursue conflicting objectives [1]. FMCW radar is attractive for sensing because it enables simple analog de-chirping and efficient multi-target range–Doppler extraction, yet it is not naturally tailored for high-throughput communications. Conversely, multicarrier waveforms offer mature equalization and high spectral efficiency, but sensing typically incurs additional processing overhead and can be sensitive in multi-target settings.

Recent work [2] introduced a practical coexistence mechanism in which an FMCW-like chirp is extracted directly from the modulator matrix (e.g., diagonal/ladder entries of the IDFT) rather than naïvely superposed, mitigating mutual interference and simplifying implementation. The same study also proposed a CP-consistent chirp-continuity method via a frequency-domain phase adjustment, enabling analog de-chirping without CP removal.

However, OFDM-based ISAC [3] can be fragile in high-mobility, doubly-dispersive channels where Doppler disrupts subcarrier orthogonality [4]. AFDM built on the discrete affine Fourier transform (DAFT), is structured to better handle delay–Doppler dispersion through quadratic phase terms in its kernel. Motivated by this property, we propose AFDM–FMCW, where an FMCW-like chirp is generated from selected entries of the inverse DAFT kernel, embedded into the AFDM modulator in a controlled manner, and stitched continuously across CP boundaries. The resulting waveform supports conventional AFDM reception for communication and standard FMCW beat-frequency processing with 2-D FFT range–Doppler estimation for sensing.

2. System Model

2.1. AFDM–FMCW Transmit Signal

Consider an AFDM block of length N with sampling period $T_s = 1/B$. Let $\mathbf{x} \in \mathbb{C}^{N\times 1}$ denote the data symbol vector. The AFDM time-domain signal is generated by the inverse DAFT (IDAFT) matrix as

$$\mathbf{s}_{\text{AFDM}} = \mathbf{A}^{-1}\mathbf{x}. \tag{1}$$

where $\mathbf{A} \in \mathbb{C}^{N\times N}$ denotes the DAFT matrix and can be written as $\mathbf{A} = \mathbf{D}_2\mathbf{F}\mathbf{D}_1$, with $\mathbf{F}$ being the N-point DFT matrix, $\mathbf{D}_1 = \text{diag}\left(e^{-j\pi c_1 n^2}\right)$ and $\mathbf{D}_2 = \text{diag}\left(e^{-j\pi c_2 n^2}\right)$ for $n = 0, \ldots, N-1$. Accordingly, $\mathbf{A}^{-1} = \mathbf{D}_1^H\mathbf{F}^H\mathbf{D}_2^H$.

An FMCW-like discrete chirp is extracted from structured entries of the IDAFT kernel using an index rule $k(n)$ (diagonal or ladder), i.e., $c[n] \triangleq \sqrt{N}\,[\mathbf{A}^{-1}]_{n,k(n)}$ for $n = 0, \ldots, N-1$, and $\mathbf{c} = [c[0], \ldots, c[N-1]]^T$. The proposed AFDM–FMCW block is

$$\mathbf{s} = \mathbf{A}^{-1}\mathbf{x} + \sqrt{\rho_c}\,\mathbf{c}, \tag{2}$$

where $\rho_c \geq 0$ controls the chirp-to-data power ratio.

2.2. CP Insertion and Channel

A CP of length L_{cp} is appended as $\tilde{\mathbf{s}} = \mathbf{T}_{\text{cp}}\mathbf{s}$. To preserve chirp continuity across blocks, the i-th block chirp is circularly shifted by iL_{cp} samples, i.e., $\mathbf{c}_i[n] = \mathbf{c}[(n - iL_{\text{cp}}) \bmod N]$.

We adopt a delay–Doppler multipath channel, where the received sample is

$$r[n] = \sum_{p=1}^{P} \alpha_p e^{j2\pi\nu_p nT_s}\tilde{s}[n - \ell_p] + w[n], \tag{3}$$

with path gain α_p, delay ℓ_p, Doppler ν_p, and noise $w[n] \sim \mathcal{CN}(0, \sigma^2)$.

2.3. Receiver Processing

After CP removal, $\mathbf{y} = \mathbf{R}_{\text{cp}}\mathbf{r}$. For communication, AFDM demodulation is performed as $\hat{\mathbf{x}} = \mathbf{A}\mathbf{y}$ followed by equalization/detection to compute the BER. For sensing, the received signal is de-chirped using the known chirp and 2-D FFT processing is applied to estimate $(\hat{R}, \hat{v})$ from the dominant spectral peak(s); RMSE_R and RMSE_v are then obtained over multiple trials.

3. Results Discussion

Simulations assume a single-target delay–Doppler channel with integer delay $\ell_p = 4$ and normalized Doppler $\nu_p = 0.1$, using $N = 256$, $L_{\text{CP}} = 32$, and bandwidth $B = 1$ GHz.

3.1. Sensing Performance

Fig. 1 compares the sensing accuracy in terms of RMSE for (a) range and (b) velocity versus SNR_c, where ρ_c is fixed (e.g., $\rho_c = 0.5$). AFDM–FMCW achieves lower RMSE across the SNR range, with a clear gain in the low-to-medium SNR regime, indicating more reliable range/velocity estimation under noisy conditions. As SNR_c increases, the RMSE decreases rapidly and then gradually approaches a similar floor for both schemes. This floor behavior is mainly attributed to finite resolution in the underlying beat-frequency/2-D FFT peak-based estimation (i.e., binning effects) rather than thermal noise. Overall, the results suggest that DAFT-kernel chirp embedding improves sensing robustness without altering the standard FMCW de-chirping and FFT-based processing.

3.2. Communication Performance

Fig. 2 shows BER versus SNR for two chirp power settings, $\rho_c \in \{0.5, 1\}$. Increasing ρ_c degrades BER because more transmit power is devoted to the FMCW component, reducing the effective power for data detection after AFDM demodulation and equalization. Importantly, for the same ρ_c, AFDM–FMCW consistently outperforms OFDM–FMCW, demonstrating improved communication robustness under the considered channel conditions. These results highlight the expected ISAC trade-off: higher chirp power benefits sensing (lower RMSE), whereas lower chirp power improves link reliability (lower BER). In practice, ρ_c can be selected to satisfy application requirements while retaining a unified transmitter and a low-complexity sensing receiver.

4. Conclusion

This paper proposes an AFDM–FMCW ISAC waveform that embeds an FMCW-like chirp into the AFDM modulator by leveraging the chirp structure inherent to the inverse DAFT kernel, inspired by transform-matrix chirp extraction and CP-consistent continuity principles reported for OFDM–FMCW. The proposed design supports (i) standard AFDM reception for communication and (ii) low-complexity FMCW de-chirping with 2-D FFT range–Doppler processing for sensing. A single control parameter ρ_c governs the sensing–communication trade-off, consistent with prior OFDM–FMCW observations. Overall, the framework is well-suited for high-mobility ISAC scenarios, offering a unified waveform and receiver architecture with low sensing complexity.

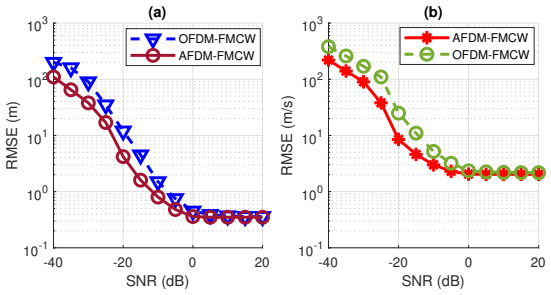

Figure 1. Sensing accuracy comparison of AFDM–FMCW and OFDM–FMCW versus SNR with fixed $\rho_c = 0.5$: (a) range RMSE and (b) velocity RMSE.

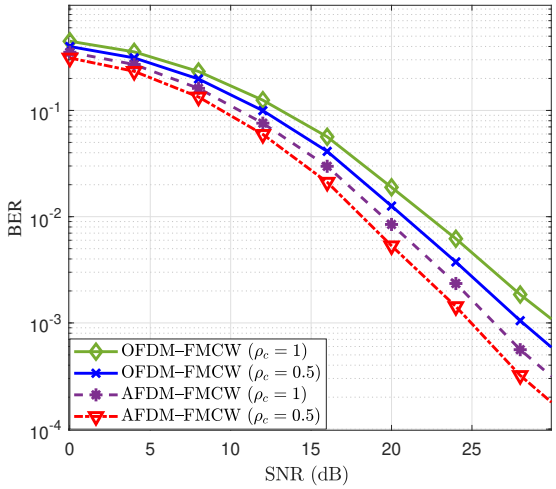

Figure 2. BER performance comparison of AFDM–FMCW and OFDM–FMCW versus SNR for $\rho_c \in \{0.5, 1\}$.

5. Acknowledgment

This work was supported by the National Research Foundation of Korea (NRF) grant funded by the Korea government (MSIT) (RS-2025-00553810, 50%). This work was supported in part by the National Research Foundation of Korea (NRF) funded by the Ministry of Science and ICT (MSIT), Korea Government under Grant (RS-2022-NR070834, 50%).

References

[1] S. Ahmad, M. Ahmad, S. Y. Shin, Dual PHY Layer Multiple Access Transceiver for Next Generation 6G Networks, in: 2024 15th International Conference on Information and Communication Technology Convergence (ICTC), 2024, pp. 1187–1192.

[2] A. Bouziane, S. Eddine Zegrar, H. Arslan, A Novel OFDM-FMCW Waveform for Low-Complexity Joint Sensing and Communication, IEEE Wireless Communications Letters 14 (2) (2025) 425–429.

[3] W. Cho, K. Chang, W. Shin, Y. Kim, Y.-J. Ko, OFDM-Based In-Band Full-Duplex ISAC Systems, IEEE Wireless Communications Letters 14 (2) (2025) 365–369.

[4] S. Ahmad, S. Y. Shin, A Novel RDC-Based Target Estimation Framework for Bistatic ISAC with AFDM-IM over Doubly-Dispersive Channels, in: Proceedings of Symposium of the Korean Institute of Communications and Information Sciences (KICS), Jeju, Republic of Korea, 2025.